nature medicine

Transcriptional regulation of endochondral ossification by HIF-2α during skeletal growth and osteoarthritis development

Taku Saito[1,2], Atsushi Fukai[1], Akihiko Mabuchi[3], Toshiyuki Ikeda[2], Fumiko Yano[4], Shinsuke Ohba[4], Nao Nishida[3], Toru Akune[5], Noriko Yoshimura[5], Takumi Nakagawa[1], Kozo Nakamura[1], Katsushi Tokunaga[3], Ung-il Chung[4] & Hiroshi Kawaguchi[1]

Chondrocyte hypertrophy followed by cartilage matrix degradation and vascular invasion, characterized by expression of type X collagen (COL10A1), matrix metalloproteinase-13 (MMP-13) and vascular endothelial growth factor (VEGF), respectively, are central steps of endochondral ossification during normal skeletal growth and osteoarthritis development. A *COL10A1* promoter assay identified hypoxia-inducible factor-2α (HIF-2α, encoded by *EPAS1*) as the most potent transactivator of *COL10A1*. HIF-2α enhanced promoter activities of *COL10A1*, *MMP13* and *VEGFA* through specific binding to the respective hypoxia-responsive elements. HIF-2α, independently of oxygen-dependent hydroxylation, was essential for endochondral ossification of cultured chondrocytes and embryonic skeletal growth in mice. HIF-2α expression was higher in osteoarthritic cartilages versus nondiseased cartilages of mice and humans. *Epas1*-heterozygous deficient mice showed resistance to osteoarthritis development, and a functional single nucleotide polymorphism (SNP) in the human *EPAS1* gene was associated with knee osteoarthritis in a Japanese population. The *EPAS1* promoter assay identified RELA, a nuclear factor-κB (NF-κB) family member, as a potent inducer of HIF-2α expression. Hence, HIF-2α is a central transactivator that targets several crucial genes for endochondral ossification and may represent a therapeutic target for osteoarthritis.

Endochondral ossification is an essential process not only for physiological skeletal growth[1], but also for development of osteoarthritis, which is the most common joint disorder and is characterized by cartilage degradation and osteophyte formation[2–7]. The process of endochondral ossification requires both the hypertrophic differentiation of chondrocytes, which is characterized by secretion of COL10A1, and the conversion of avascular cartilage tissue into highly vascularized bone tissue via degradation of the cartilage matrix and vascular invasion[1,8]. The matrix degradation requires proteinases, among which MMP-13 has a major role[8,9], and the vascular invasion depends on an angiogenic switch by VEGF[8,10]. These steps of chondrocyte hypertrophy, cartilage degradation and vascular invasion are well coordinated; however, the molecular mechanism that extensively controls the sequential steps remains an enigma. Here we initially performed a screen of transcription factors that potentiate the expression of *COL10A1* and identify HIF-2α, an α-subunit member of the HIF family, as the most potent transactivator.

The HIF protein family consists of α- and β-subunit members that function by forming heterodimers[11]. Under normoxic conditions, the α-subunit members HIF-1α, HIF-2α and HIF-3α undergo oxygen-dependent hydroxylation, resulting in ubiquitination and degradation by the proteasome[12,13]. In contrast, under hypoxic conditions, they are neither hydroxylated nor degraded, and they heterodimerize with the constitutive β-subunit members known as aryl hydrocarbon receptor nuclear translocator (ARNT), ARNT2, ARNT-like (ARNTL) and ARNTL2. The heterodimers activate transcription of the target genes by binding the consensus sequence called hypoxia-responsive element (HRE) in the promoters[11]. As cartilage is an avascular and hypoxic tissue, HIF proteins may have a crucial role in the functions of chondrocytes, and, in fact, HIF-1α is known be a potent regulator of cartilage homeostasis[14–16]. However, HIF-2α and HIF-1α are not functionally redundant[17–21], and little is known about the function of HIF-2α in chondrocytes. Here we examined the role of HIF-2α in endochondral ossification during skeletal growth and osteoarthritis development and investigate the underlying mechanism.

RESULTS

Identification of HIF-2α as a transactivator of *COL10A1*

We initially performed a screen of transcription factors that induce hypertrophic differentiation using mouse chondrogenic ATDC5 cells and human nonchondrogenic HeLa cells transfected with a proximal promoter fragment of the *COL10A1* gene. For candidate molecules, we

[1]Sensory & Motor System Medicine, University of Tokyo, Hongo, Bunkyo-ku, Tokyo, Japan. [2]Bone and Cartilage Regenerative Medicine, University of Tokyo, Hongo, Bunkyo-ku, Tokyo, Japan. [3]Human Genetics, University of Tokyo, Hongo, Bunkyo-ku, Tokyo, Japan. [4]Center for Disease Biology and Integrative Medicine, University of Tokyo, Hongo, Bunkyo-ku, Tokyo, Japan. [5]22nd Century Medical and Research Center, Faculty of Medicine, University of Tokyo, Hongo, Bunkyo-ku, Tokyo, Japan. Correspondence should be addressed to H.K. (kawaguchi-ort@h.u-tokyo.ac.jp).

Received 10 February; accepted 8 March; published online 23 May 2010; doi:10.1038/nm.2146

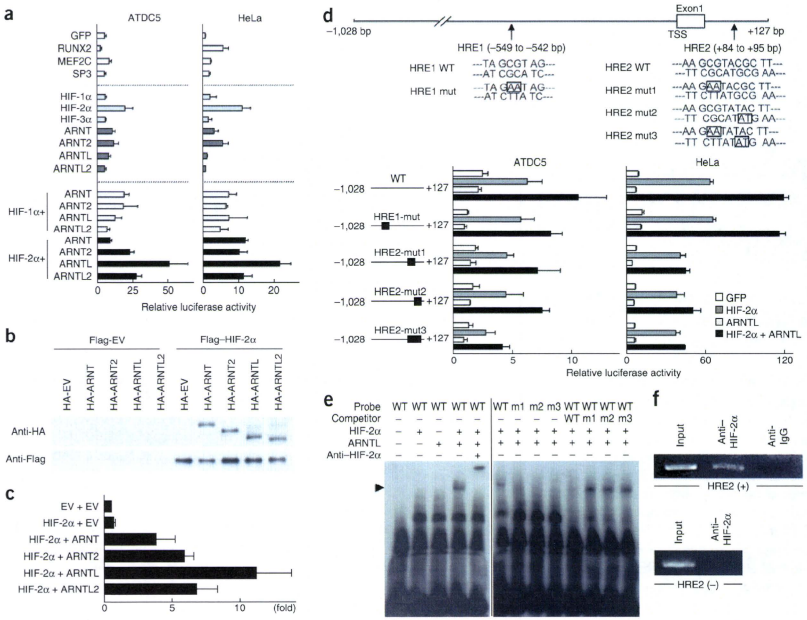

Figure 1 Transcriptional regulation of *COL10A1* by HIF-2α. (**a**) Luciferase assay for screening transcription factors that activate the *COL10A1* promoter by the transfections of candidate genes into ATDC5 and HeLa cells with a reporter construct containing a fragment (−1,028 to +127 bp) of the *COL10A1* gene. Data are shown as means ± s.d. (**b**) Immunoprecipitation and immunoblotting analysis by co-transfections of Flag-tagged HIF-2α or the control empty vector (EV) and hemagglutinin (HA)-tagged β-subunit members or the EV in ATDC5 cells. (**c**) Mammalian two-hybrid assay by transfections of vectors expressing GAL4–HIF-2α and VP16–β-subunit fusion proteins with the luciferase reporter vector with GAL4 binding sites into HeLa cells. Data are shown as means ± s.d. of relative fold increase in luciferase activity as compared to EV + EV (which is arbitrarily set to 1). (**d**) Site-directed mutagenesis analyses of the luciferase assay; one in HRE1 and three in HRE2 (+87 and +88 for mut1, +91 and +92 for mut2, and both for mut3), in the two cell lines transfected with GFP, HIF-2α, ARNTL or both HIF-2α and ARNTL. Data are shown as means ± s.d. (**e**) EMSA for specific binding (arrowhead) of the wild-type (WT) oligonucleotide probe containing HRE2 or the mutated probes described in **d** (m1, m2 and m3) with *in vitro*–translated HIF-2α, ARNT or both. Supershift by an antibody to HIF-2α (anti–HIF-2α) and cold competition with a 50-fold excess of unlabeled WT or the mutated probe are presented. (**f**) ChIP assay with cell lysates of human chondrogenic SW1353 cells that were amplified by a primer set spanning the HRE2 (+, +32 to +249 bp) or not spanning the HRE2 (−, −2,131 to −1,900 bp) before (input) and after immunoprecipitation with anti-HIF-2α or nonimmune IgG (anti-IgG).

prepared expression vectors of more than 100 transcription factors that are known to be expressed in chondrocytes, including HIF proteins, runt-related transcription factor-2 (RUNX2)[1,22], myocyte enhancer factor-2C (MEF2C)[23] and specificity protein-3 (SP3)[24] (**Fig. 1a**). Among them, HIF-2α showed the strongest activation in both cell lines. Although all β-subunit members were physically associated with HIF-2α in ATDC5 cells (**Fig. 1b**), ARNTL showed the strongest binding affinity to HIF-2α (**Fig. 1c**), and HIF-2α–ARNTL was the most potent combination for *COL10A1* transactivation (**Fig. 1a**).

In the *COL10A1* promoter, we identified two HREs by the consensus sequence [A/G]CGT (ref. 25), one in the 5′-end flanking region (HRE1) and the other in intron 1 (HRE2) (**Fig. 1d**). We introduced mutations in HRE1 and HRE2, but only the latter mutation resulted in suppression of transactivation by HIF-2α and the HIF-2α–ARNTL combination (**Fig. 1d**). We then confirmed the specific binding of the HIF-2α protein to HRE2 by electrophoretic mobility shift assay (EMSA) and chromatin immunoprecipitation (ChIP) assay (**Fig. 1e,f**).

HIF protein expression during chondrocyte differentiation

Although the HIF α- and β-subunit members were widely expressed in major tissues of adult mice, *Epas1* was most predominantly expressed in the tracheal cartilage (**Supplementary Fig. 1a**). During differentiation of ATDC5 cells, *Epas1* expression increased in accordance with the three representative factors for central steps of endochondral ossification: *Col10a1*, *Mmp13* and *Vegfa*, whereas *Hif1a* expression was strong at the early stage and decreased thereafter (**Fig. 2a**). *Hif3a* expression was very low, and the β-subunit members were extensively expressed in all differentiation stages (**Fig. 2a**).

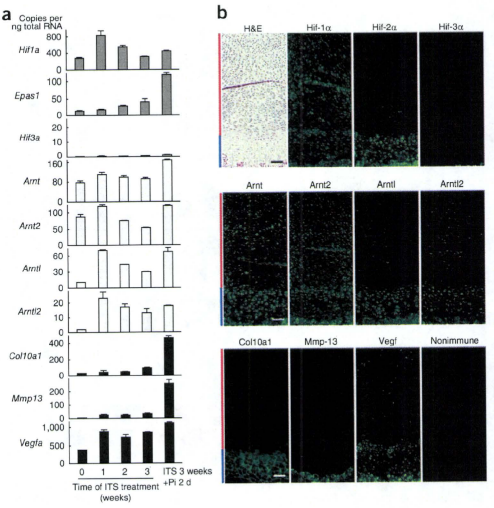

Figure 2 *In vitro* and *in vivo* expression patterns of the HIF α- and β-subunit members and Col10a1, Mmp-13 and Vegf during chondrocyte differentiation. (**a**) Time course of mRNA levels of the indicated genes during differentiation of mouse chondrogenic ATDC5 cells cultured with ITS (insulin, transferrin and sodium selenite) for 3 weeks and for 2 d more with inorganic phosphate (Pi). Data are expressed as means ± s.d. (**b**) H&E staining and immunofluorescence with antibodies to the indicated proteins, as well as a nonimmune control, in the proximal tibias of mouse embryos (embryonic day 18.5 (E18.5)). Scale bars, 100 μm. Red and blue bars to the left of each row indicate layers of proliferative and hypertrophic zones, respectively.

In tibial limb cartilage of mouse embryos, Hif-2α was localized primarily in the hypertrophic zone, similarly to Col10a1, Mmp-13 and Vegf (**Fig. 2b**). In contrast, Hif-1α was predominantly localized in chondrocytes at earlier differentiation stages in the proliferative zone, and Hif-3α was hardly detectable (**Fig. 2b**). The localizations of Arntl and Arntl2 were similar to Hif-2α, whereas those of Arnt and Arnt2 were similar to Hif-1α (**Fig. 2b**).

Physiological role of HIF-2α in endochondral ossification

To determine the involvement of HIF-2α in skeletal growth, we investigated the skeletal phenotype of *Epas1*-deficient mice. The homozygous deficient mutants (*Epas1*$^{-/-}$) were extraordinarily small and died at the early embryonic stage, as reported previously[20,21] (**Fig. 3a**). Although the heterozygous deficient mutants (*Epas1*$^{+/-}$) developed and grew without abnormalities of major organs, they showed mild but proportional dwarfism compared to wild-type littermates from embryonic stages up to 1 week after birth (**Fig. 3a,b** and **Supplementary Fig. 1b**). In the embryos, the limbs and vertebrae were 7–16% shorter in *Epas1*$^{+/-}$ mice than in the wild-type littermates (**Fig. 3c**). Although the actual length of the proliferative zone of the *Epas1*$^{+/-}$ limb was comparable to that of wild-type, the percentage of the proliferative zone relative to the total limb length was moderately increased (**Fig. 3d,e**) with normal BrdU-positive proliferative cells but suppressed Col10a1 expression (**Fig. 3f,g**), indicating impaired hypertrophic differentiation without an effect on proliferation caused by Hif-2α insufficiency. The percentage of the hypertrophic zone relative to the total limb length was also increased and that of the bone area was considerably decreased in the *Epas1*$^{+/-}$ limbs (**Fig. 3d,e**), indicating that Hif-2α insufficiency impaired not only chondrocyte hypertrophy but also subsequent steps such as matrix degradation and vascularization. This difference was gradually decreased with developmental compression of the hypertrophic zone after birth (**Supplementary Fig. 1c**). Immunohistochemistry confirmed that Mmp-13 and Vegf, as well as Col10a1, were suppressed by the Hif-2α insufficiency, which may cause the decrease in cartilage calcification shown by von Kossa staining (**Fig. 3f**).

Function of HIF-2α in cultured chondrocytes

In cultured ATDC5 cells, *Col10a1*, *Mmp13* and *Vegfa* amounts, as well as the activity of alkaline phosphatase and Alizarin red staining (both indicators of differentiation), were increased by overexpression of HIF-2α or the HIF-2α–ARNTL combination, whereas none of the expression levels or staining was affected by ARNTL alone (**Fig. 4a**). To examine the regulation of HIF-2α function by oxygen-dependent hydroxylation, we created ATDC5 lines overexpressing four kinds of HIF-2α mutants bearing mutations at the oxygen-dependent hydroxylation residues, including N847A and P531A (or both), which result in enhancement of the transactivation activity of the protein even under normoxic conditions, as well as P849A, which abrogates transactivation activity even under hypoxic conditions[13]. We found that none of these mutations affected the HIF-2α action on endochondral ossification parameters (**Fig. 4b**). All parameters were decreased, however, by loss of function of HIF-2α in ATDC5 cells achieved through overexpression of a dominant-negative mutant or expression of an siRNA specific for HIF-2α (**Fig. 4c**). In addition to ATDC cells, primary chondrocytes derived from *Epas1*$^{+/-}$ mice showed suppressed expression of the three factors, and the suppression of each factor was restored to wild-type levels by adenoviral overexpression of HIF-2α (**Fig. 4d**).

We then examined the transcriptional regulation of *MMP13* and *VEGFA* by HIF-2α. Among the α- and β-subunit members of the HIF proteins, HIF-2α most notably transactivated both *MMP13* and *VEGFA*, and the transactivation was further enhanced by ARNTL (**Supplementary Fig. 2a,b**), as is true for *COL10A1* (**Fig. 1a**). Deletion and site-directed mutagenesis analyses of the luciferase assay identified the core responsive elements to HIF-2α and the HIF-2α–ARNTL combination at HRE3 (−106 to −101) and HRE4 (−982 to −977) in the promoters of *MMP13* and *VEGFA*, respectively (**Supplementary Fig. 2c,d**). Further EMSA and ChIP assays confirmed the specific binding of the HIF-2α protein to HRE3 and HRE4 (**Supplementary Fig. 2e–h**).

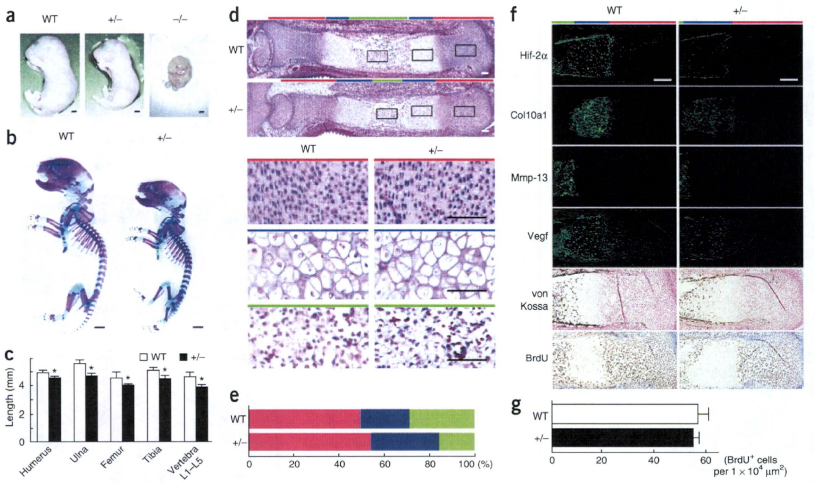

Figure 3 Skeletal abnormality in *Epas1*-deficient mice. (**a**) Wild-type (WT), heterozygous-deficient (*Epas1*$^{+/-}$) and homozygous-deficient (*Epas1*$^{-/-}$) littermate embryos (E17.5). All *Epas1*$^{-/-}$ embryos died at mid-gestation. Scale bars, 1 mm. (**b**) Double staining with Alizarin red and Alcian blue of the whole skeleton of WT and *Epas1*$^{+/-}$ littermate embryos (E17.5). Scale bars, 1 mm. (**c**) Length of long bones and vertebra (first to fifth lumbar spines) of WT and *Epas1*$^{+/-}$ littermate embryos. Data are expressed as means ± s.d. *$P < 0.05$ versus WT. (**d**) H&E staining of whole tibias of the WT and *Epas1*$^{+/-}$ littermate embryos. Inset boxes indicate the regions of the bottom three rows representing proliferative zone, hypertrophic zone and bone area, shown by red, blue and green bars, respectively. Scale bars, 100 μm. (**e**) Percentage of the length of proliferative zone (red), hypertrophic zone (blue) and bone area (green) over the total tibial length of the WT and *Epas1*$^{+/-}$ littermate embryos. (**f**) Immunofluorescence with antibodies to Hif-2α, Col10a1, Mmp-13 and Vegf, as well as bromodeoxyuridine (BrdU) labeling and von Kossa staining of the proximal tibias of WT and *Epas1*$^{+/-}$ littermate embryos (E17.5). Color bars indicate layers as indicated in **d**. Scale bars, 200 μm. (**g**) The number of BrdU-positive cells in 1×10^4 μm^2 of the proximal tibia of WT and *Epas1*$^{+/-}$ littermate embryos. Data are expressed as means ± s.d.

Contribution of HIF-2α to osteoarthritis in mice and humans

We next compared osteoarthritis development between adult littermates of wild-type and *Epas1*$^{+/-}$ mice that had undergone comparable skeletal growth after birth (**Supplementary Fig. 1b**) by creating a surgical osteoarthritis model through induction of instability to the knee joints[4,5]. The expression of Hif-2α, as well as of Col10a1, Mmp-13 and Vegf, increased in the joint cartilage with osteoarthritis development for 8 weeks after surgery in the wild-type mice; however, in the *Epas1*$^{+/-}$ littermates, the cartilage degradation and the expression of the three factors were notably suppressed (**Fig. 5a**). Quantification by grading systems[4,26] confirmed that the Hif-2α insufficiency caused significant resistance to cartilage degradation and osteophyte formation (**Fig. 5b**). There was no difference in the subchondral bones between the two genotypes under the sham operation, suggesting that the *Epas1* deficiency does not affect physiological bone homeostasis. However, after surgical induction, subchondral bone sclerosis, an osteoarthritic disorder secondary to cartilage destruction, was apparent in the wild-type joints, whereas it was suppressed in the *Epas1*$^{+/-}$ joints (**Supplementary Table 1**).

In human knee joint samples, as well, the HIF-2α expression increased with osteoarthritis development, reached a maximum at the initial and progressive stages and decreased thereafter at the terminal stage, although it was hardly detected in subchondral bone or synovium (**Fig. 5c**). To further investigate a possible association of the human *EPAS1* gene with knee osteoarthritis of humans, we searched a Japanese population–based cohort of the ROAD study[27] for sequence variations in exons and the 5′-end flanking region up to −1,000 bp from the transcription start site (TSS) of the human *EPAS1* gene and identified only one common SNP with a minor allele frequency >0.1, rs17039192 (+18C and +18T for major and minor alleles, respectively, relative to the TSS; minor allele frequency = 0.132) (**Fig. 5d**). A comparison of allelic frequencies between 397 individuals with knee osteoarthritis and 437 controls showed significant association of the rs17039192 SNP with knee osteoarthritis ($P = 0.013$, odds ratio = 1.44) (**Fig. 5d**). Because this SNP was located close to the TSS, we further examined the effects of the allelic difference (+18C/T) on *EPAS1* promoter activity in chondrogenic and nonchondrogenic cells transfected with a luciferase reporter gene and the *EPAS1* promoter fragment (−1,000 bp to 488 bp) containing +18C or +18T. The susceptibility allele (18C) showed higher promoter activity in chondrogenic cells, but not in nonchondrogenic cells (**Fig. 5e**), confirming that enhanced transactivation of *EPAS1* in chondrocytes is associated with osteoarthritis in humans.

Molecular network around HIF-2α in endochondral ossification

Regarding downstream molecules of HIF-2α, we have focused on COL10A1, MMP-13 and VEGF as representative factors for the

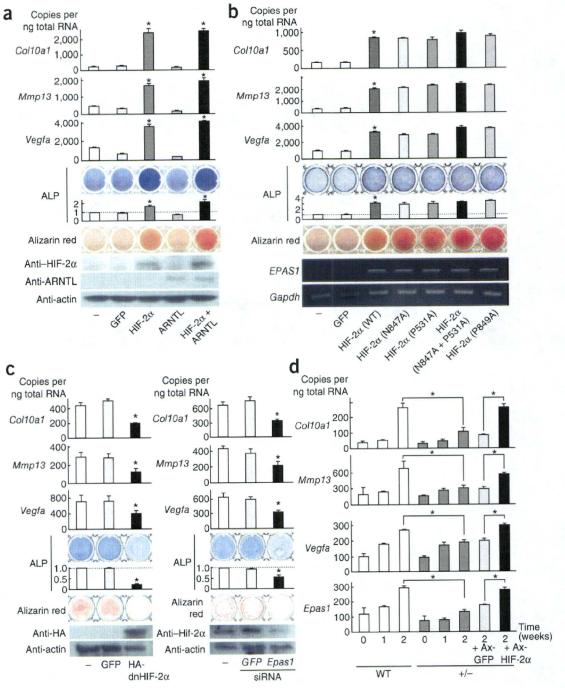

Figure 4 Effects of gain and loss of function of HIF-2α on endochondral ossification parameters in cultures of chondrogenic cells. (**a**) mRNA levels of *Col10a1*, *Mmp13* and *Vegfa*, alkaline phosphatase (ALP) activity (relative to control) and Alizarin red staining in stable lines of ATDC5 cells retrovirally transfected with GFP, HIF-2α, ARNTL or both HIF-2α and ARNTL and in nontransfected parental cells (–) after culture for 3 weeks with ITS and 2 d with Pi. HIF-2α and ARNTL levels were confirmed by western blotting, with the actin level as the internal control. (**b**) Analyses of the parameters in **a** in stable ATDC5 lines transfected with GFP or HIF-2α mutants at the oxygen-dependent hydroxylation residues causing enhancement (N847A and P531A) and abrogation (P849A) of HIF-2α transactivation activity under the culture conditions used in **a**. Gene expression was confirmed by RT-PCR with the *EPAS1* primer set inside the coding sequence, with the *Gapdh* level as the internal control. (**c**) Analyses of the same read-outs in **a** in stable ATDC5 lines transfected with GFP or HA-tagged dominant-negative HIF-2α (HA–dnHIF-2α) (left) or siRNA specific for *GFP* or *Epas1* mRNA (right) under the cultures conditions used in **a**. HA–dnHIF-2α and Hif-2α amounts were confirmed by western blotting. (**d**) mRNA levels of *Col10a1*, *Mmp13* and *Vegfa* and *Epas1* in the pellet cultures of primary chondrocytes derived from wild-type (WT) and *Epas1*$^{+/-}$ littermate embryos for 2 weeks. For the rescue experiment, adenoviral transfection with HIF-2α (Ax–HIF-2α) or the control GFP (Ax-GFP) was performed before the pellet formation. All data are expressed as means ± s.d. $^*P < 0.05$ versus GFP unless otherwise indicated.

central three steps of endochondral ossification (chondrocyte hypertrophy, cartilage degradation and vascularization) and found that all were the direct transcriptional targets. However, there are other factors related to endochondral ossification, including in the earlier cartilage formation step and in the later osteogenesis step, which might also be targets of HIF-2α. We therefore examined the expression patterns of the following factors: type II collagen (COL2A1) and aggrecan (AGC1) as cartilage matrix proteins; RUNX2, Indian hedgehog (IHH), and type 1 PTH/PTHrP receptor (PTH1R) as chondrocyte hypertrophy markers; MMP-3, MMP-9, a disintegrin and metalloproteinase with thrombospondin type 1 motif-4 (ADAMTS4) and ADAMTS5 as cartilage-degradable proteinases; and type I collagen (COL1A1), bone sialoprotein (BSP), osteocalcin, alkaline phosphatase, bone morphogenetic protein-2 (BMP-2), BMP-4 and BMP-7 as osteogenic markers. In cultured ATDC5 cells, expression of chondrocyte hypertrophy markers, cartilage degradable proteinases and osteogenic markers increased in accordance with the cell differentiation and *Epas1* expression (**Supplementary Fig. 3a**). The chondrocyte hypertrophy markers and cartilage degradable proteinases were localized mainly in the hypertrophic zone of the mouse limb cartilage, similarly to Hif-2α (**Supplementary Fig. 3b**). The mRNA levels of cartilage matrix proteins, chondrocyte hypertrophy markers and most of the osteogenic markers were increased in ATDC5 cells overexpressing HIF-2α or HIF-2α–ARNTL (**Supplementary Fig. 4a**). Among cartilage-degradable proteinases, expression of *Mmp3* and *Mmp9* was increased, whereas neither *Adamts4* nor *Adamts5* was affected (**Supplementary Fig. 4a**). In contrast, mRNA levels of the chondrocyte hypertrophy markers *Mmp3* and *Mmp9* were decreased after overexpression of a dominant-negative mutant form of HIF-2α and siRNA specific for *Epas1* mRNA in ATDC5 cells (**Supplementary Fig. 4b,c**); however, cartilage matrix proteins, *Adamts4*, *Adamts5* and most of osteogenic markers were little affected. Primary chondrocytes derived from *Epas1*$^{+/-}$ mice reproducibly showed suppression of the chondrocyte hypertrophy markers, *Mmp3* and *Mmp9*, but not cartilage matrix proteins, *Adamts4*, *Adamts5* or osteogenic factors, and the suppression was restored to wild-type levels by HIF-2α overexpression (**Supplementary Fig. 5**). Further *in vivo* analyses of embryonic limbs (**Supplementary Fig. 6a**) and osteoarthritic knee joints (**Supplementary Fig. 6b**) confirmed the decreases in expression of the chondrocyte hypertrophy markers, Mmp-3 and Mmp-9, but not cartilage matrix proteins Adamts4 or Adamts5, by Hif-2α insufficiency. HIF-2α enhanced the promoter activities of the chondrocyte hypertrophy markers *MMP3* and *MMP9*, as well as *Col10a1*, *Mmp13*, and *Vegfa* mRNA levels, much more strongly than HIF-1α, and the stimulation of the mRNA levels by HIF-2α was not altered by cotransfection of

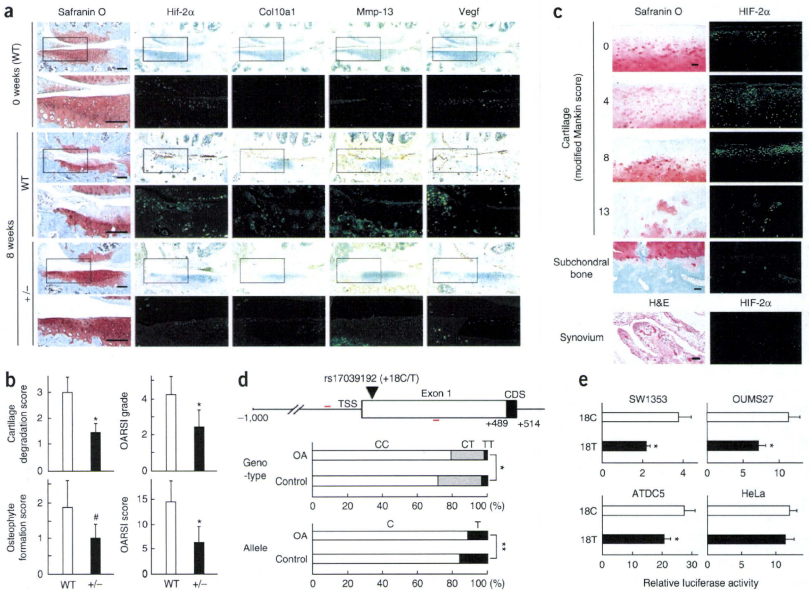

Figure 5 Contribution of HIF-2α to osteoarthritis development in mice and humans. (**a**) Cartilage degradation assessed by safranin O staining and expression of Hif-2α, Col10a1, Mmp-13 and Vegf by immunostaining (brown) and immunofluorescence (green) in mouse knee joints 0 and 8 weeks after creating a surgical osteoarthritis model in 8-week-old wild-type (WT) and *Epas1*$^{+/-}$ littermates. Boxed areas in each safranin O–stained or each immunostained image indicate the regions shown in the enlarged safranin O–stained or immunofluorescent image immediately below. Scale bars, 100 μm. (**b**) Quantification of osteoarthritis development by our (two left graphs) and OARSI (two right graphs) grading systems. Data are expressed as means ± s.d. #$P < 0.05$, *$P < 0.01$ versus WT. (**c**) Safranin O staining, H&E staining and immunofluorescence with an antibody to HIF-2α in human tibial cartilages of various degradation stages, subchondral bone (beneath the cartilage with Mankin score = 8) and synovium (around the cartilage with Mankin score = 8), obtained as surgical specimens of total knee arthroplasty. Scale bars, 100 μm. (**d**) Top, the identified SNP, rs17039192, and primers used for genotyping (red lines) in the human *EPAS1* gene. CDS, coding sequence. Bottom, association of the rs17039192 (+18C/T) SNP with knee osteoarthritis (OA) diagnosed on radiographs using the Kellgren/Lawrence grade in a Japanese population. The odds ratio of the susceptibility allele was 1.44 (95% confidence interval: 1.08–1.92). *$P = 0.05$, **$P = 0.013$. (**e**) Luciferase activities in chondrogenic SW1353, OUMS27 and ATDC5 cells and nonchondrogenic HeLa cells transfected with a luciferase reporter gene construct ligated to a fragment (−1,000 bp to +488 bp) containing +18C or +18T. Data are shown as means ± s.d. *$P < 0.05$ versus 18C.

HIF-1α (**Supplementary Fig. 7a,b**). Furthermore, the endochondral ossification parameters stimulated by HIF-2α overexpression in ATDC5 cells were not inhibited by suppression of RUNX2 through overexpression of a dominant-negative mutant RUNX2 (**Supplementary Fig. 7c**).

Finally, to identify the upstream mechanism that regulates HIF-2α, we performed a screen of transcription factors with the *EPAS1* promoter fragment including the +18C SNP described above. Among candidate molecules that are known to regulate chondrocyte differentiation, such as sex-determining region Y box (SOX), RUNX, CCAAT/enhancer binding protein (C/EBP), MEF2, SP/Kruppel-like factor (KLF), activating transcription factor (ATF), cAMP responsive element–binding protein (CREB), Notch and NF-κB family members, we found that v-rel reticuloendotheliosis viral oncogene homolog A (RELA or NF-κB p65), an essential molecule of the NF-κB signal, showed the strongest activation in all cells (**Fig. 6a**). In the *EPAS1* promoter we identified an NF-κB motif and found that site-directed mutagenesis in the motif caused suppression of transactivation by RELA (**Fig. 6b**). The allelic difference (+18C/T) of the rs17039192 SNP described above also altered the activation of *EPAS1* promoter by RELA but did not affect it when the NF-κB motif was mutated, suggesting the involvement of this SNP in the *EPAS1* transactivation and osteoarthritis development caused by the NF-κB signal. We further confirmed that the proinflammatory cytokines tumor necrosis factor-α (TNF-α) and interleukin-1β (IL-1β), putative inducers of the NF-κB signal[28], increased *EPAS1* expression in cultured chondrogenic cells (**Fig. 6c**). In mouse knee joint cartilage, the expression of Rela was increased during osteoarthritis development, similarly to Hif-2α expression (**Fig. 6d**).

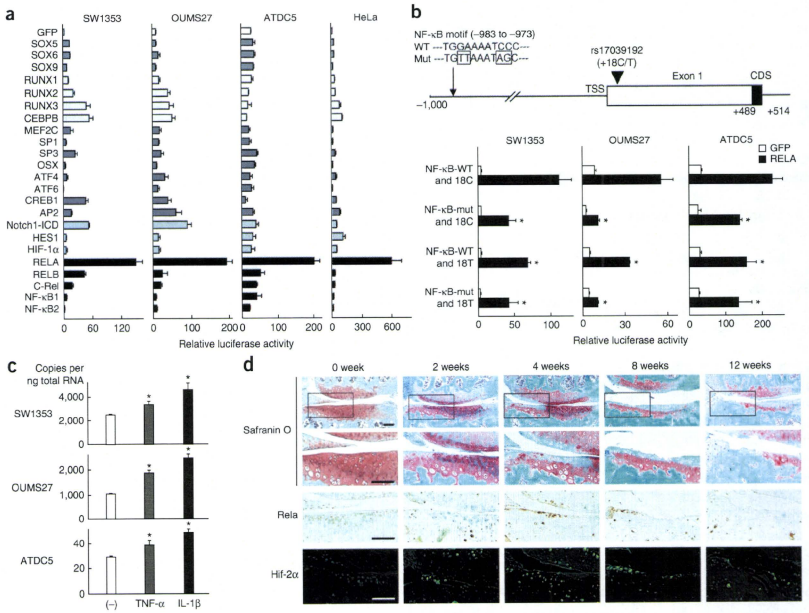

Figure 6 Upstream mechanism that regulates HIF-2α. (**a**) Luciferase activities after transfections of putative chondrocyte-related transcription factors into chondrogenic SW1353, OUMS27 and ATDC5 cells and nonchondrogenic HeLa cells with a reporter construct containing a fragment (−1,000 bp to +488 bp) of the *EPAS1* gene. OSX, osterix; AP2, transcription factor AP-2α; Notch1-ICD, intercellular domain of Notch1; HES1, hairy and enhancer of split 1. Data are shown as means ± s.d. (**b**) Top, depiction of the NF-κB motif (−983 to −973) in the human *EPAS1* gene. Bottom, site-directed mutagenesis analyses of the luciferase assay in the three chondrogenic cell lines transfected with GFP or RELA. Luciferase activities were compared with or without mutation in the NF-κB motif and with +18C or +18T of the rs17039192 SNP. Data are shown as means ± s.d. $^*P < 0.05$ versus wild-type NF-κB and 18C with RELA. (**c**) mRNA levels of *EPAS1* in the three chondrogenic cells cultured with or without TNF-α or IL-1β (each 1 ng ml^{-1}) for 2 d. Data are expressed as means ± s.d. $^*P < 0.05$ versus control. (**d**) Time course of degradation in mouse knee joint cartilage, as shown by Safranin O staining and expression of Rela and Hif-2α by immunostaining and immunofluorescence, respectively, in a surgical osteoarthritis model in 8-week-old mice. Boxed areas in each of the top images are enlarged in the bottom images directly beneath. Scale bar, 100 μm.

DISCUSSION

Among the sequential steps of endochondral ossification—cartilage formation, chondrocyte hypertrophy, cartilage degradation, vascularization and osteogenesis—this study reveals that HIF-2α functions as an extensive transcriptional regulator of the central three steps. HIF-2α shares about 50% amino acid homology with HIF-1α (ref. 20), a potent regulator of cartilage homeostasis[14–16]; however, accumulating evidence has shown distinct expression patterns and functions between the two HIF proteins[17–21]. HIF-1α is expressed mainly in hypovascular and hypoxic tissues[16,19,29], whereas HIF-2α is expressed even in vascularized tissues[11,29]. In cartilage as well, previous studies and our current study show that HIF-1α is expressed from the early stage of cartilage formation, and its activity is enhanced by hypoxia[13–16,30]. In contrast, HIF-2α is expressed mainly in highly differentiated chondrocytes, and its function is independent of oxygen-dependent hydroxylation. Likewise, although cartilage-specific knockout of HIF-1α leads to defects in the earlier stage of cartilage formation and the later stage of chondrocyte survival and osteogenesis[14–16], *Epas1*$^{+/-}$ mice show growth retardation with defects in the central steps of endochondral ossification. Hence, HIF-1α and HIF-2α may have distinct roles via different mechanisms: hypoxia-dependent cartilage formation and maintenance by HIF-1α and less hypoxia-dependent endochondral ossification by HIF-2α. We have also confirmed that neither gain nor loss of function of HIF-2α alters HIF-1α expression during chondrocyte differentiation, nor does HIF-1α transfection affect *EPAS1* promoter activity. Furthermore, HIF-1α hardly stimulates the expression of markers of the central steps of endochondral ossification in the presence or absence of HIF-2α, indicating independent functions of HIF-1α and HIF-2α at least in the central steps. However, we do not deny the possibility of interactions between HIF-1α and HIF-2α in earlier and later stages of endochondral ossification. The HIF-2α function may possibly be compensated by HIF-1α in this earlier stage, as cartilage matrix proteins are not altered by HIF-2α suppression. In the later or severe stage of osteoarthritic

cartilage, expression of HIF-2α decreases after reaching a maximum at the initiation of cartilage degradation in mice and humans, as was reported in a previous study[31]. In this terminal stage, the decreased HIF-2α expression may enhance autophagy in mature chondrocytes of osteoarthritic cartilage, as HIF-2α is known to antagonize the autophagy-accelerator function of HIF-1α[32].

Our study reveals that *COL10A1*, *MMP13* and *VEGFA* are the direct transcriptional targets of HIF-2α. The functional relationships *in vivo* are supported by previous reports that a deficiency of *Mmp13* or *Vegfa* in mice causes a skeletal phenotype similar to that in *Epas1*$^{+/-}$ mice, with elongation of the hypertrophic zone and delay of ossification in the limb cartilage[9,10], although the skeletal phenotypes of *Col10a1*-knockout mice differs among the reports[33–35]. Our further studies identify *RUNX2*, *IHH*, *PTH1R*, *MMP3* and *MMP9* as possible transcriptional targets of HIF-2α. We have recently reported that HIF-2α enhances *Runx2* promoter activity[36] and that *Runx2*$^{+/-}$ mice show resistance to osteoarthritis development under mechanical instability, similarly to *Epas1*$^{+/-}$ mice[5]. However, HIF-2α and RUNX2 may promote endochondral ossification via independent mechanisms.

There are two mechanisms of osteoarthritis protection: induction of anabolism or inhibition of catabolism in joint cartilage. The protection in *Epas1*$^{+/-}$ mice is not likely to be due to induction of anabolism, as the anabolic markers COL2A1 and AGC1 are unaffected in joint cartilage. Although recent studies have identified ADAMTS5 and related molecules as key catabolic regulators of osteoarthritis development[37–40], neither ADAMTS4 nor ADAMTS5 is regulated by HIF-2α, implicating another pathway. Because *Mmp13*$^{-/-}$ mice are reported to be protected from cartilage degradation despite considerable aggrecan loss after surgical osteoarthritis induction[41], similarly to *Epas1*$^{+/-}$ mice, the osteoarthritis protection caused by the Hif-2α insufficiency might occur principally through regulation of Mmp-13.

Suppression of osteoarthritis development was obvious in *Epas1*$^{+/-}$ mice, whereas skeletal growth retardation was mild and transient, suggesting that pathological endochondral ossification is more dependent on HIF-2α than is physiological endochondral ossification. As a trigger of osteoarthritis, mechanical stress may induce the upstream NF-κB signal and HIF-2α expression in joint cartilage, which causes endochondral ossification by transactivation of *COL10A1*, *MMP13*, *VEGFA* and other factors. Recent comprehensive profiling analyses of not only genes and proteins, but also microRNAs, is unraveling the molecular network underlying osteoarthtitis development[42]; however, we hereby propose that signals in the HIF-2α axis from NF-κB signaling to endochondral ossification–related molecules may represent a rational therapeutic target for osteoarthritis with minimal effects on physiological skeletal homeostasis.

METHODS

Methods and any associated references are available in the online version of the paper at http://www.nature.com/naturemedicine/.

Note: Supplementary information is available on the Nature Medicine website.

ACKNOWLEDGMENTS

We thank R. Yamaguchi and H. Kawahara for technical assistance. This study was supported by a grant-in-aid for Scientific Research from the Japanese Ministry of Education, Culture, Sports, Science and Technology (19109007 and 20689028). The sponsor had no role in study design, data collection, data analysis, data interpretation or writing of the manuscript.

AUTHOR CONTRIBUTIONS

T.S., T.I. and H.K. performed project planning; T.S., A.F., A.M., F.Y. and S.O. performed the experiments; T.S., A.M., N.N., T.A., N.Y., T.N., K.N., K.T., U.-i.C. and H.K. conducted data analysis; T.S. and H.K. wrote the manuscript.

COMPETING FINANCIAL INTERESTS

The authors declare no competing financial interests.

Published online at http://www.nature.com/naturemedicine/.
Reprints and permissions information is available online at http://npg.nature.com/reprintsandpermissions/.

1. Kronenberg, H.M. Developmental regulation of the growth plate. *Nature* **423**, 332–336 (2003).
2. Kühn, K., D'Lima, D.D., Hashimoto, S. & Lotz, M. Cell death in cartilage. *Osteoarthritis Cartilage* **12**, 1–16 (2004).
3. Kawaguchi, H. Endochondral ossification signals in cartilage degradation during osteoarthritis progression in experimental mouse models. *Mol. Cells* **25**, 1–6 (2008).
4. Kamekura, S. *et al.* Osteoarthritis development in novel experimental mouse models induced by knee joint instability. *Osteoarthritis Cartilage* **13**, 632–641 (2005).
5. Kamekura, S. *et al.* Contribution of runt-related transcription factor 2 to the pathogenesis of osteoarthritis in mice after induction of knee joint instability. *Arthritis Rheum.* **54**, 2462–2470 (2006).
6. Yamada, T. *et al.* Carminerin contributes to chondrocyte calcification during endochondral ossification. *Nat. Med.* **12**, 665–670 (2006).
7. Drissi, H., Zuscik, M., Rosier, R. & O'Keefe, R. Transcriptional regulation of chondrocyte maturation: potential involvement of transcription factors in OA pathogenesis. *Mol. Aspects Med.* **26**, 169–179 (2005).
8. Ortega, N., Behonick, D.J. & Werb, Z. Matrix remodeling during endochondral ossification. *Trends Cell Biol.* **14**, 86–93 (2004).
9. Stickens, D. *et al.* Altered endochondral bone development in matrix metalloproteinase 13–deficient mice. *Development* **131**, 5883–5895 (2004).
10. Zelzer, E. *et al.* VEGFA is necessary for chondrocyte survival during bone development. *Development* **131**, 2161–2171 (2004).
11. Semenza, G.L. HIF-1 and human disease: one highly involved factor. *Genes Dev.* **14**, 1983–1991 (2000).
12. Schofield, C.J. & Ratcliffe, P.J. Oxygen sensing by HIF hydroxylases. *Nat. Rev. Mol. Cell Biol.* **5**, 343–354 (2004).
13. Lando, D., Peet, D.J., Whelan, D.A., Gorman, J.J. & Whitelaw, M.L. Asparagine hydroxylation of the HIF transactivation domain a hypoxic switch. *Science* **295**, 858–861 (2002).
14. Pfander, D., Cramer, T., Schipani, E. & Johnson, R.S. HIF-1α controls extracellular matrix synthesis by epiphyseal chondrocytes. *J. Cell Sci.* **116**, 1819–1826 (2003).
15. Schipani, E. Hypoxia and HIF-1α in chondrogenesis. *Ann. NY Acad. Sci.* **1068**, 66–73 (2006).
16. Schipani, E. *et al.* Hypoxia in cartilage: HIF-1α is essential for chondrocyte growth arrest and survival. *Genes Dev.* **15**, 2865–2876 (2001).
17. Patel, S.A. & Simon, M.C. Biology of hypoxia-inducible factor-2α in development and disease. *Cell Death Differ.* **15**, 628–634 (2008).
18. O'Rourke, J.F., Tian, Y.M., Ratcliffe, P.J. & Pugh, C.W. Oxygen-regulated and transactivating domains in endothelial PAS protein 1: comparison with hypoxia-inducible factor-1α. *J. Biol. Chem.* **274**, 2060–2071 (1999).
19. Jain, S., Maltepe, E., Lu, M.M., Simon, C. & Bradfield, C.A. Expression of ARNT, ARNT2, HIF1 α, HIF2 α and Ah receptor mRNAs in the developing mouse. *Mech. Dev.* **73**, 117–123 (1998).
20. Tian, H., Hammer, R.E., Matsumoto, A.M., Russell, D.W. & McKnight, S.L. The hypoxia-responsive transcription factor EPAS1 is essential for catecholamine homeostasis and protection against heart failure during embryonic development. *Genes Dev.* **12**, 3320–3324 (1998).
21. Scortegagna, M. *et al.* Multiple organ pathology, metabolic abnormalities and impaired homeostasis of reactive oxygen species in *Epas1*$^{-/-}$ mice. *Nat. Genet.* **35**, 331–340 (2003).
22. Komori, T. Regulation of skeletal development by the Runx family of transcription factors. *J. Cell. Biochem.* **95**, 445–453 (2005).
23. Arnold, M.A. *et al.* MEF2C transcription factor controls chondrocyte hypertrophy and bone development. *Dev. Cell* **12**, 377–389 (2007).
24. Magee, C., Nurminskaya, M., Faverman, L., Galera, P. & Linsenmayer, T.F. SP3/SP1 transcription activity regulates specific expression of collagen type X in hypertrophic chondrocytes. *J. Biol. Chem.* **280**, 25331–25338 (2005).
25. Pescador, N. *et al.* Identification of a functional hypoxia-responsive element that regulates the expression of the egl nine homologue 3 (egln3/phd3) gene. *Biochem. J.* **390**, 189–197 (2005).
26. Pritzker, K.P. *et al.* Osteoarthritis cartilage histopathology: grading and staging. *Osteoarthritis Cartilage* **14**, 13–29 (2006).
27. Muraki, S. *et al.* Prevalence of radiographic knee osteoarthritis and its association with knee pain in the elderly of Japanese population–based cohorts: the ROAD study. *Osteoarthritis Cartilage* **17**, 1137–1143 (2009).
28. Li, Q. & Verma, I.M. NF-κB regulation in the immune system. *Nat. Rev. Immunol.* **2**, 725–734 (2002).
29. Stewart, A.J., Houston, B. & Farquharson, C. Elevated expression of hypoxia inducible factor-2α in terminally differentiating growth plate chondrocytes. *J. Cell. Physiol.* **206**, 435–440 (2006).
30. Amarilio, R. *et al.* HIF1α regulation of Sox9 is necessary to maintain differentiation of hypoxic prechondrogenic cells during early skeletogenesis. *Development* **134**, 3917–3928 (2007).

31. Bohensky, J. *et al.* Regulation of autophagy in human and murine cartilage: hypoxia-inducible factor 2 suppresses chondrocyte autophagy. *Arthritis Rheum.* **60**, 1406–1415 (2009).
32. Srinivas, V., Bohensky, J., Zahm, A.M. & Shapiro, I.M. Autophagy in mineralizing tissues: microenvironmental perspectives. *Cell Cycle* **8**, 391–393 (2009).
33. Gress, C.J. & Jacenko, O. Growth plate compressions and altered hematopoiesis in collagen X null mice. *J. Cell Biol.* **149**, 983–993 (2000).
34. Kwan, K.M. *et al.* Abnormal compartmentalization of cartilage matrix components in mice lacking collagen X: implications for function. *J. Cell Biol.* **136**, 459–471 (1997).
35. Rosati, R. *et al.* Normal long bone growth and development in type X collagen–null mice. *Nat. Genet.* **8**, 129–135 (1994).
36. Tamiya, H. *et al.* Analysis of the Runx2 promoter in osseous and non-osseous cells and identification of HIF2A as a potent transcription activator. *Gene* **416**, 53–60 (2008).
37. Echtermeyer, F. *et al.* Syndecan-4 regulates ADAMTS-5 activation and cartilage breakdown in osteoarthritis. *Nat. Med.* **15**, 1072–1076 (2009).
38. Glasson, S.S. *et al.* Deletion of active ADAMTS5 prevents cartilage degradation in a murine model of osteoarthritis. *Nature* **434**, 644–648 (2005).
39. Lin, A.C. *et al.* Modulating hedgehog signaling can attenuate the severity of osteoarthritis. *Nat. Med.* **15**, 1421–1425 (2009).
40. Stanton, H. *et al.* ADAMTS5 is the major aggrecanase in mouse cartilage in vivo and in vitro. *Nature* **434**, 648–652 (2005).
41. Little, C.B. *et al.* Matrix metalloproteinase 13-deficient mice are resistant to osteoarthritic cartilage erosion but not chondrocyte hypertrophy or osteophyte development. *Arthritis Rheum.* **60**, 3723–3733 (2009).
42. Iliopoulos, D., Malizos, K.N., Oikonomou, P. & Tsezou, A. Integrative microRNA and proteomic approaches identify novel osteoarthritis genes and their collaborative metabolic and inflammatory networks. *PLoS One* **3**, e3740 (2008).

ONLINE METHODS

Cell cultures. We cultured HeLa (Riken BRC), OUMS27 (the Health Science Research Resources Bank) and SW1353 (American Type Culture Collection) cells in DMEM with 10% FBS and ATDC5 cells (Riken BRC) in DMEM and F12 (1:1) with 5% FBS, and we performed experiments using these cell lines as previously described[43]. We used TNF-α and IL-1β (Peprotech) at final concentrations of 1 ng ml^{-1} for 2 d.

Construction of expression vectors. We prepared expression vectors for the luciferase assay and for co-immunoprecipitation in pCMV-HA (Clontech) and pCMV-3Tag-1A (Stratagene), respectively, and created the dnRUNX2, dnHIF-2α and HIF-2α mutants at the oxygen-dependent hydroxylation residues as previously described[13,44,45]. We constructed an siRNA vector for the mouse *Epas1* gene (nucleotides 1,140–1,160) with piGENEmU6 vector (iGENE Therapeutics)[46] and pMx vectors[47], retrovirus vectors using pMx vectors[47,48], adenovirus vectors by the AdenoX Expression system (Clontech), and we verified all vectors by DNA sequencing.

Luciferase assay. We prepared the *COL10A1* promoter region (from −1,028 to +127 bp relative to the TSS), *MMP13* (−1,000 to 0), *VEGFA* (−1,000 to 0), *RUNX2* (−1,480 to 0), *IHH* (−1,488 to 0), *PTH1R* (−1,529 to 0), *MMP3* (−1,551 to +39), *MMP9* (−1,775 to +17) and *EPAS1* (−1,000 to +488) by PCR using human genomic DNA as the template, and we cloned them into the pGL3-Basic vector or the pGL4.10[luc2] vector (Promega). We created deletion and mutation constructs by PCR, performed luciferase assays with the Dual-Luciferase Reporter Assay System (Promega) and showed the data as the ratio of the firefly activities to the *Renilla* activities.

Co-immunoprecipitation and mammalian two-hybrid assays. We performed co-immunoprecipitation with EZ view Red Protein A and anti-FLAG M2 Affinity Gels (Sigma) and mammalian two-hybrid assays with the Checkmate mammalian two-hybrid system (Promega).

Electrophoretic mobility shift assay. We prepared HIF-2α and ARNTL proteins by *in vitro* translation with the TNT T7 Quick System (Promega) and the pCITE4 vector (Novagen), and we performed the EMSA with the DIG Gel Shift Kit (Roche). Regions of the oligonucleotide probe were as follows: *COL10A1*, from +70 to +111 bp relative to the TSS; *MMP13*, −125 to −81; *VEGFA*, −1,002 to −957.

Chromatin immunoprecipitation assay. We performed the ChIP assay in SW1353 cells with a OneDay ChIP kit (Diagenode). For immunoprecipitation, we used antibodies to HIF-2α (Santa Cruz Biotechnology) and the normal rabbit IgG (Invitrogen). Primer sets, one spanning and the other not spanning the identified enhancer element, are as follows: *COL10A1*, +32 to +249 and −2,131 to −1,900; *MMP13*, −214 to −29 and −4,797 to −4,551; *VEGFA*, −1,000 to −795 and −4,685 to −4,507, respectively.

Mice. We purchased Hif-2α–mutant mice[20] from the Jackson Laboratory. In each experiment, we compared male *Epas1*$^{+/-}$ and wild-type littermates. We performed all experiments according to a protocol approved by the Animal Care and Use Committee of the University of Tokyo. We isolated primary chondrocytes from the ribs of mouse embryos, cultured them in a monolayer for 2 d and in a pellet for additional 2 weeks in DMEM with 10% FBS and transduced adenoviruses at 100 multiplicities of infection 4 h before the pellet formation.

Osteoarthritis experiment. We performed the surgical procedure to create an experimental osteoarthritis model on 8-week-old male mice as previously reported[4–6], and we analyzed them 8 weeks after surgery. We quantified osteoarthritis severity by our original grading system[4] and by the OARSI system (0–6 for grade and 0–24 for score)[26], which was assessed by a single observer who was blinded to the experimental group. We performed histomorphometric measurements in eight optical fields of the subchondral bones, according to the American Society for Bone and Mineral Research nomenclature report[49].

Human samples. We obtained human samples from individuals undergoing total knee arthroplasty after obtaining written informed consent as approved by the Ethics Committee of the University of Tokyo. We histologically assessed cartilage samples with the modified Mankin scoring system[50,51].

Case-control association study. We recruited individuals over 50 years of age with (n = 397; mean age, 75.6; range, 53–89) and without (n = 437; mean age, 73.6; range, 60–87) knee osteoarthritis in a population-based cohort of the ROAD study[27]. We diagnosed osteoarthritis on the basis of radiographic findings by the Kellgren-Lawrence grading system[52]: the knee osteoarthritis population included individuals with grades 3 and 4 and the control population with grades 0 and 1. After obtaining written informed consent as approved by the Ethics Committee of the University of Tokyo, we extracted genomic DNA from peripheral blood leukocytes of individuals using standard protocols. We searched SNPs around the *EPAS1* gene using the dbSNP database, and we genotyped the identified SNP by PCR restriction fragment length polymorphism (RFLP) using BanI as the enzyme. We confirmed that the P value of the Hardy-Weinberg equilibrium test in the control population was higher than 0.01.

Other analyses. We performed real-time RT-PCR, western blotting and histological analyses as previously reported[48,53]. Primer sequences and antibody information are available upon request.

Statistical analyses. We performed statistical analyses of experimental data with the unpaired two-tailed Student's t test. In the case control association study, we evaluated genotypic and allelic models by the χ^2 test for the Hardy-Weinberg equilibrium using spreadsheet software (Excel). P values less than 0.05 were considered significant.

43. Saito, T., Ikeda, T., Nakamura, K., Chung, U.I. & Kawaguchi, H. S100A1 and S100B, transcriptional targets of SOX trio, inhibit terminal differentiation of chondrocytes. *EMBO Rep.* **8**, 504–509 (2007).
44. Maemura, K. *et al.* Generation of a dominant-negative mutant of endothelial PAS domain protein 1 by deletion of a potent C-terminal transactivation domain. *J. Biol. Chem.* **274**, 31565–31570 (1999).
45. Ueta, C. *et al.* Skeletal malformations caused by overexpression of Cbfa1 or its dominant negative form in chondrocytes. *J. Cell Biol.* **153**, 87–100 (2001).
46. Miyagishi, M. & Taira, K. RNAi expression vectors in mammalian cells. *Methods Mol. Biol.* **252**, 483–491 (2004).
47. Kitamura, T. New experimental approaches in retrovirus-mediated expression screening. *Int. J. Hematol.* **67**, 351–359 (1998).
48. Morita, S., Kojima, T. & Kitamura, T. Plat-E: an efficient and stable system for transient packaging of retroviruses. *Gene Ther.* **7**, 1063–1066 (2000).
49. Parfitt, A.M. *et al.* Bone histomorphometry: standardization of nomenclature, symbols, and units. Report of the ASBMR Histomorphometry Nomenclature Committee. *J. Bone Miner. Res.* **2**, 595–610 (1987).
50. Mankin, H.J., Dorfman, H., Lippiello, L. & Zarins, A. Biochemical and metabolic abnormalities in articular cartilage from osteo-arthritic human hips. II. Correlation of morphology with biochemical and metabolic data. *J. Bone Joint Surg. Am.* **53**, 523–537 (1971).
51. Ostergaard, K., Andersen, C.B., Petersen, J., Bendtzen, K. & Salter, D.M. Validity of histopathological grading of articular cartilage from osteoarthritic knee joints. *Ann. Rheum. Dis.* **58**, 208–213 (1999).
52. Kellgren, J.H. & Lawrence, J.S. Radiological assessment of osteo-arthrosis. *Ann. Rheum. Dis.* **16**, 494–502 (1957).
53. Hirata, M. *et al.* C/EBPβ promotes transition from proliferation to hypertrophic differentiation of chondrocytes through transactivation of p57. *PLoS One* **4**, e4543 (2009).

J Orthop Sci (2010) 15:14–19
DOI 10.1007/s00776-009-1412-1

JOURNAL OF
ORTHOPAEDIC SCIENCE

Original article

Analysis of interobserver reliability for radiographic staging of coxarthrosis and indexes of acetabular dysplasia: a preliminary study

Yoshio Takatori[1], Kazuya Ito[2], Muroto Sofue[3], Yoshio Hirota[2], Moritoshi Itoman[4], Tadami Matsumoto[5], Yoshiki Hamada[6], Hiroyuki Shindo[7], Harumoto Yamada[8], Yuji Yasunaga[9], Hiroshi Ito[10], Satoshi Mori[11], Ichiro Owan[12], Genji Fujii[13], Hirotsugu Ohashi[14], Taro Mawatari[15], Toshiro Iga[3], Naonobu Takahira[4], Tanzo Sugimori[5], Hajime Sugiyama[6], Kunihiko Okano[7], Tatsuro Karita[16], Kenichi Ando[8], Takanari Hamaki[9], Teruhisa Hirayama[10], Ken Iwata[17], Masanori Matsuura[14], and Seiya Jingushi[18] for the Investigation Group into Coxarthrosis and Acetabular Dysplasia in Japan

[1] Division of Science for Joint Reconstruction, Graduate School of Medicine, The University of Tokyo, Tokyo, Japan
[2] Department of Public Health, Osaka City University Graduate School of Medicine, Osaka, Japan
[3] Orthopaedic Division, Nakajo Central Hospital, Niigata, Japan
[4] Department of Orthopedic Surgery, School of Medicine, Kitasato University, Sagamihara, Japan
[5] Department of Orthopaedic Surgery, Kanazawa Medical University, Uchinada, Japan
[6] Interdisciplinary Graduate School of Medicine and Engineering, University of Yamanashi, Chuo, Japan
[7] Department of Orthopaedic Surgery, Graduate School of Medicine, Nagasaki University, Nagasaki, Japan
[8] Department of Orthopaedic Surgery, Fujita Health University, School of Medicine, Toyoake, Japan
[9] Department of Artificial Joints and Biomaterials, Graduate School of Biomedical Sciences, Hiroshima University, Hiroshima, Japan
[10] Department of Orthopaedic Surgery, Asahikawa Medical College, Asahikawa, Japan
[11] Department of Bone and Joint Surgery, Seirei Hamamatsu General Hospital, Hamamatsu, Japan
[12] Orthopaedic Surgery, Department of Clinical Neuroscience, School of Medicine, University of the Ryukyus, Nishihara, Japan
[13] Tohoku Hip Joint Center, Matuda Hospital, Sendai, Japan
[14] Department of Orthopedic Surgery, Saiseikai Nakatsu Hospital, Osaka, Japan
[15] Department of Orthopaedic Surgery, Graduate School of Medical Sciences, Kyushu University, Fukuoka, Japan
[16] Orthopaedic Surgery, Sensory and Motor System Medicine, Surgical Sciences, Graduate School of Medicine, The University of Tokyo, Tokyo, Japan
[17] Department of Orthopaedic Surgery, Kagawa University Faculty of Medicine, Miki, Japan
[18] Department of Orthopaedic Surgery, Kyushu Rosai Hospital of Japan Labour Health and Welfare Organization, 1-3-1 Takamatsu Kuzuhara, Kokura-minami-ku, Kitakyushu 800-0296, Japan

Abstract

Background. We are planning a multicenter survey on coxarthrosis and acetabular dysplasia in Japan. To collect reliable data, we performed a preliminary study to elucidate the observer agreement on assessment items.

Methods. We collected radiographs of hip joints in eight patients with various findings of coxarthrosis. Twelve registered orthopedic specialists evaluated them regarding the roentgenographic stage of coxarthrosis and five indexes of acetabular dysplasia (acetabular angle, center-edge angle, acetabular roof obliquity, acetabular head quotient, approximate acetabular quotient). To assess observer agreement, we calculated the value of the kappa statistic for stages and the coefficient of variation for the indexes. The same 12 specialists then assessed the coxarthritis stage on the same radiographs 1 month after the first evaluation based on our own descriptions of the roentgenographic stages.

Results. For the first evaluation of the roentgenographic stage, the value of the kappa statistic was 0.448; and for the second evaluation it was 0.600. The results of the coefficient of variation for the indexes of acetabular dysplasia, ranked in ascending order, were as follows: acetabular angle, acetabular head quotient, acetabular roof obliquity, center-edge angle, approximate acetabular quotient.

Conclusions. For the upcoming multicenter survey, clear descriptions of the stages of coxarthrosis and selection of appropriate indexes can be helpful for collecting dependable results.

Offprint requests to: S. Jingushi
Received: July 4, 2008/ Accepted: August 24, 2009

Introduction

Coxarthrosis is one of the major diseases that affect the healthy life-span of a population. To take systematic measures against it, we should know the actual situation of patients. There are, however, no nationwide data on this disorder in Japan. Hence, we are preparing a multicenter survey under the direction of one of the authors of this article (S.J.). Because many cases of coxarthrosis are considered to be secondary to acetabular dysplasia in this country,[1] we are including not only roentgenographic stages of coxarthrosis but also indexes of acetabular dysplasia in the assessment. Before undertaking

such a large study and owing to the need for reliable data from the many institutions, it was necessary to examine the reproducibility of the roentgenographic stage classification and the acetabular dysplasia indexes. We therefore conducted this preliminary study of observer agreement on these items because there had been no such studies to investigate the issue previously.

Materials and methods

Study 1

One of the authors collected radiographs of the hip joints of eight patients with various radiological findings of coxarthrosis. These films had been obtained in his hospital with patients in a supine position. The target–film distance was 100 cm, and the X-ray beam was directed to the proximal margin of the symphysis pubis. Personal information was deleted, and a set of duplicate films were sent to 12 institutions: one in the Hokkaido region, one in the Tohoku region, two in the Kanto region, four in the Chubu region, one in the Chugoku-Shikoku region, and three in the Kyushu region. At each institution, one of the authors, a registered orthopedic specialist, evaluated the stage of coxarthrosis[2] and calculated five indexes of acetabular dysplasia: acetabular angle,[3] center-edge (CE) angle,[4] acetabular roof obliquity,[5] acetabular head quotient (AHQ),[6] approximate acetabular quotient (AAQ).[6] Approval was given by the institutional review board to use the radiographs of hip osteoarthritis patients that had been obtained previously.

To determine the stage of coxarthrosis, we employed the classification proposed by the Japanese Orthopaedic Association's (JOA) committee on evaluation criteria for this condition (Table 1).[2] It defined five groups: almost normal, prearthrosis, initial stage, advanced stage, terminal stage. The committee focused on three roentgenographic features: the width of the joint space, the structure of the bony architecture, the shape of the acetabular roof and the femoral head. There was, however, no description of groups or an authorized English translation.

Of the roentgenographic indexes of acetabular dysplasia, we used the line connecting bilateral teardrops as the transverse baseline for measurement. To measure the acetabular angle, the CE angle, the acetabular roof obliquity, and the AAQ, we identified the edge of the acetabular roof. When there was a spur at the lateral margin of the acetabulum, we did not employ the tip of the spur as a measuring point. Instead, we extended the lateral line of the ilium just proximal to the acetabulum distally and defined the point at the intersection with the sourcil as the lateral edge of the acetabulum.[7]

One of the authors, whose institution did not participate in film reading, performed the statistical analysis. For the stage of coxarthrosis, he computed the value of the kappa statistic[8] and evaluated the strength of observer agreement.[9] For the roentgenographic indexes, he set up a mixed linear model to calculate the coefficient of variation. In this model, the observer was viewed as a random effect, whereas the case, composite of the film number and the side, and the stage were viewed as fixed effects. Based on this premise, he calculated the coefficient of variation using the analysis of variance (ANOVA). When observers agreed well on the measurement of a certain index, its value of the coefficient of variation was small.

Study 2

To overcome the difficulty of staging coxarthrosis, we defined the stages from our own point of view and selected typical radiographs for reference (Table 2, Fig. 1). On the basis of this arrangement, the same 12 authors assessed the roentgenographic stage on the same radiographs again 1 month after Study 1.

Table 1. JOA staging criteria for coxarthrosis

Stage[a]	Joint space	Bony architecture	Shape of the acetabular roof and the femoral head
0	Almost normal	Almost no change	Almost normal
1	Slight incongruity, no narrowing	Changes in trabeculae	Congenital or acquired morphological change
2	Incongruity, partial narrowing	Sclerosis of the acetabulum	Small osteophyte
3	Incongruity, localized contact of the subchondral bones	Sclerosis of the acetabulum, bone cyst(s) in the acetabulum or the femoral head	Steophyte, bone formation on the acetabular floor
4	Incongruity, extensive disappearance of the joint space	Extensive sclerosis, large bone cyst(s)	Prominent osteophyte(s), double floor, destruction of the acetabulum

Translated by the authors from the original Japanese (ref. 2)
JOA, Japanese Orthopaedic Association
[a] 0, almost normal; 1, prearthrosis; 2, initial stage; 3, advanced stage; 4, terminal stage

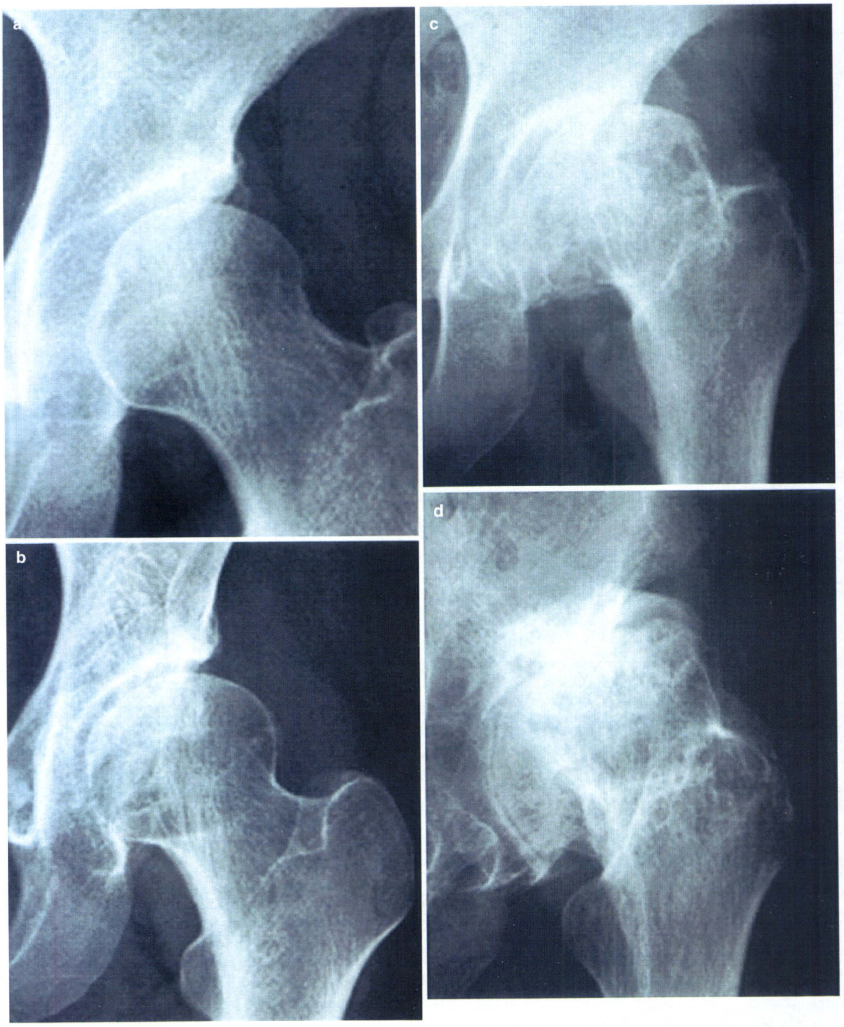

Fig. 1. Plain radiographs of the hip joint as references for staging coxarthrosis. **a** Prearthrosis. **b** Initial stage. **c** Advanced stage. **d** Terminal stage. (From Jingushi S. Osteoarthritis of hips. In: Sugioka Y, Iwamoto Y, editors. Jinnaka's textbook of orthopaedic surgery. Tokyo: Nanzando; 2004. p. 809. With permission)

Table 2. Roentgenographic stages of coxarthrosis defined by the authors

Stage	Description
Prearthrosis	No arthrotic changes.[a] Morphological changes of the acetabulum and/or proximal femur related to osteoarthrosis.[b]
Initial stage	One or more arthrotic changes. Possible narrowing of joint space. The width of joint space is maintained 2 mm or more throughout the weight-bearing area.
Advanced stage	Definite narrowing of joint space. The width is less than 2 mm at the thinnest point. Loss of joint space[c] is observed, and the width is less than 15 mm.
Terminal stage	Gross loss of joint space; the width is 15 mm or more.

[a] Arthrotic changes: joint space narrowing, sclerosis, cyst formation, and osteophytes
[b] Morphological changes related to osteoarthrosis: acetabular dysplasia, femoral head deformity such as coxa plana, subluxation, and dislocation
[c] Loss of joint space: the subchondral bone of the acetabulum is in contact with that of the femoral head

Table 3. Number of answers to roentgenograhic stages (Study 1)

Film no.	Side	Stage[a]					
		0	0 or 1	1	2	3	4
1	Rt	0	2	5	4	0	0
1	Lt	0	1	7	3	0	0
2	Rt	8	3	0	0	0	0
2	Lt	0	0	0	0	7	4
3	Rt	5	3	1	2	0	0
3	Lt	0	0	1	2	8	0
4	Rt	0	0	0	1	10	0
4	Lt	0	0	1	9	1	0
5	Rt	0	0	0	8	3	0
5	Lt	5	2	3	1	0	0
6	Rt	5	3	3	0	0	0
6	Lt	1	3	7	0	0	0
7	Rt	0	0	0	0	0	11
7	Lt	7	3	0	1	0	0
8	Rt	8	2	0	1	0	0
8	Lt	5	2	2	2	0	0

[a] See Table 1

Fig. 2. Film no. 1, right hip joint. Five researchers classified this hip joint as prearthrosis, four as the initial stage, and two as "almost normal or prearthrosis"

Results

Study 1

Roentgenographic stages of coxarthrosis

Eleven researchers reported their first evaluations (Table 3). Disagreement was most apparent among the three groups of almost normal, prearthrosis, and the initial stage. Moreover, two or three observers classified nine hips as "almost normal or prearthrosis" (Fig. 2). Considering the power of statistical analysis, we dealt with these two categories as one unit. Consequently, the kappa statistic was calculated as 0.448, and the strength of agreement was evaluated as "moderate." [9]

Roentgenographic indexes of acetabular dysplasia

All 12 researchers reported their first evaluations (Table 4). The value of the coefficient of variation was smallest for the acetabular angle and increased in the following order: AHQ, acetabular roof obliquity, CE angle, AAQ (Fig. 3). Thus, the observers had more agreement on the acetabular angle than on the CE angle, which are two representative indexes.

Study 2

All 12 researchers reported their results (Table 5). In this study, all researchers classified each hip as one of the five groups. The value of the kappa statistic was calculated as 0.600, and the strength of agreement was evaluated as "moderate." [9]

Discussion

We found that the kappa statistic for the roentgenographic stage was as small as 0.448 in Study 1. This may

Table 4. Roentgenographic indexes of acetabular dysplasia

Film no.	Side	Indexes				
		Acetabular angle	Center-edge angle	Acetabular roof obliquity	Acetabular head quotient	Approximate acetabular quotient
1	Rt	46.4 ± 2.1	10.8 ± 3.8	26.8 ± 1.4	0.65 ± 0.04	0.19 ± 0.04
1	Lt	43.2 ± 2.5	15.4 ± 3.7	20.2 ± 1.8	0.69 ± 0.06	0.21 ± 0.05
2	Rt	40.8 ± 1.1	29.7 ± 2.3	10.4 ± 4.3	0.83 ± 0.03	0.26 ± 0.04
2	Lt	51.2 ± 3.3	−14.5 ± 19.0	40.9 ± 3.9	0.43 ± 0.11	0.07 ± 0.02
3	Rt	39.3 ± 2.2	27.0 ± 7.4	3.5 ± 5.9	0.79 ± 0.04	0.30 ± 0.05
3	Lt	51.3 ± 3.8	−0.75 ± 8.2	32.1 ± 4.4	0.51 ± 0.07	0.16 ± 0.03
4	Rt	49.6 ± 4.0	5.5 ± 7.3	33.8 ± 8.4	0.58 ± 0.08	0.21 ± 0.05
4	Lt	49.3 ± 3.3	9.6 ± 5.1	26.3 ± 2.7	0.60 ± 0.05	0.22 ± 0.03
5	Rt	40.5 ± 1.5	15.7 ± 6.1	21.2 ± 4.6	0.69 ± 0.03	0.18 ± 0.04
5	Lt	41.2 ± 2.6	24.6 ± 5.7	12.6 ± 2.7	0.82 ± 0.02	0.23 ± 0.04
6	Rt	41.3 ± 2.4	26.3 ± 4.5	8.5 ± 1.7	0.79 ± 0.02	0.26 ± 0.03
6	Lt	46.5 ± 2.6	18.6 ± 1.6	16.8 ± 1.3	0.70 ± 0.02	0.25 ± 0.04
7	Rt	45.9 ± 1.4	2.8 ± 5.2	13.3 ± 13.5	0.53 ± 0.03	0.21 ± 0.04
7	Lt	42.3 ± 2.9	30.6 ± 4.1	8.4 ± 5.6	0.85 ± 0.02	0.29 ± 0.09
8	Rt	38.8 ± 2.3	24.9 ± 4.3	10.1 ± 1.4	0.81 ± 0.04	0.23 ± 0.03
8	Lt	38.5 ± 2.0	27.4 ± 3.9	8.9 ± 3.1	0.81 ± 0.04	0.25 ± 0.03

Results are the mean ± standard deviation

Fig. 3. Film no. 2, left hip joint. The acetabular angle was reported to be 51.2° ± 3.3°, and the CE angle was −14.5° ± 19.0°

be attributed to two causes. First, the researchers were trained in different centers. Fujii et al.[10] performed a similar study using orthopedic surgeons who were trained in the same university hospital. They reported the value of the kappa statistic as 0.541. Second, the classification proposed by the JOA committee[2] bears the intrinsic ambiguity of the roentgenographic stage.

Table 5. Number of answers to roentgenograhic stages (Study 2)

Film no.	Side	Stage[a]					
		0	0 or 1	1	2	3	4
1	Rt	0	3	7	2	0	0
1	Lt	0	1	6	5	0	0
2	Rt	7	3	2	0	0	0
2	Lt	0	0	0	0	9	3
3	Rt	5	1	1	5	0	0
3	Lt	0	0	0	4	8	0
4	Rt	0	0	0	0	12	0
4	Lt	0	0	0	10	2	0
5	Rt	0	0	0	10	2	0
5	Lt	5	2	3	2	0	0
6	Rt	4	3	5	0	0	0
6	Lt	1	3	8	0	0	0
7	Rt	0	0	0	0	0	12
7	Lt	6	2	0	4	0	0
8	Rt	6	3	2	1	0	0
8	Lt	4	3	3	2	0	0

[a] See Table 1

In fact, several registered orthopedic specialists found it difficult to distinguish the almost normal hip and the hip with prearthrosis. To eliminate ambiguity over the classification, we referred to preceding studies[11,12] and then defined the stages from our own point of view. For example, we described the initial stage as the state in which the reduced joint space is maintained ≥2 mm throughout the weight-bearing area. Although the setting of ≥2 mm is arbitrary, we regarded the virtual existence of the articular cartilage as essential to draw a distinction between the initial stage and the advanced

stage. We also employed a width of 15 mm loss of joint space as a provisional boundary value between the advanced stage and the terminal stage. These refinements substantially improved observer agreement in Study 2. Our intention here is to define a modified classification so we can collect dependable results in our own multiinstitutional study; it is not to propose a new classification for general use.

Regarding the roentgenographic indexes of acetabular dysplasia, we obtained an unexpectedly large value for the coefficient of variation for the CE angle, one of the most popular indexes. This is probably due to the fact that we should determine the center of the femoral head to measure it. Whereas Wiberg showed radiographs in which the femoral head was round,[4] several radiographs in our study showed heads that were severely deformed. According to the coefficient of variation values, the acetabular angle, AHQ, and acetabular oblique angle are more reliable for multicenter surveys than the CE angle or AHQ.

It is our belief that a clear description of the stages of coxarthrosis and selection of appropriate indexes can be helpful for collecting dependable results in our upcoming multicenter survey.

Acknowledgments. This study was supported by grants from the Japanese Orthopaedic Association and the Japanese Hip Society.

The authors did not or will not receive any benefits from any commercial party related directly or indirectly to the subject of this article.

References

1. Nakamura S, Ninomiya S, Nakamura T. Primary osteoarthritis of the hip joint in Japan. Clin Orthop 1999;241:190–6.
2. Ueno R. Staging of osteoarthritis of the hip joint according to the roentgenographic findings. J Jpn Orthop Assoc 1971;45:826–8 (in Japanese).
3. Sharp IK. Acetabular dysplasia: the acetabular angle. J Bone Joint Surg Br 1961;43:268–72.
4. Wiberg G. Studies on dysplastic acetabula and congenital subluxation of the hip joint with special reference to the complication of osteoarthritis. Acta Chir Scand Suppl 1939;58:1–135.
5. Massie WK, Howorth MB. Congenital dislocation of the hip. Part I. Method of grading results. J Bone Joint Surg Am 1950;32: 519–31.
6. Heyman CH, Herndon CH. Legg-Perthes disease: a method for the measurement of the roentgenographic result. J Bone Joint Surg Am 1950;32:767–8.
7. Miura T. Studies on roentgenographic changes of the normal hip joint in adult with the age. J Jpn Orthop Assoc 1971;45:703–14 (in Japanese).
8. Cohen J. A coefficient of agreement for nominal scales. Educ Psychol Meas 1960;20:37–46.
9. Landis JR, Koch GG. The measurement of observer agreement for categorical data. Biometrics 1977;33:159–74.
10. Fujii G, Nakayama A, Seki M, Maeda S, Chiba T, Yamada N, et al. The reliability of JOA classification of osteoarthritis of the hip joint. Hip Joint 1998;24:381–5 (in Japanese).
11. Tonnis D. Congenital dysplasia and dislocation of the hip in children and adults. 1st edn. Tokyo: Springer; 1987. p. 167.
12. Okano K, Enomoto H, Shindo H. Assessment for the patients with total hip arthroplasty after rotational acetabular osteotomy. Hip Joint 2005;31:76–9 (in Japanese).

J Orthop Sci (2010) 15:626–631
DOI 10.1007/s00776-010-1507-8

JOURNAL OF
ORTHOPAEDIC SCIENCE
© The Japanese Orthopaedic Association

Original Article

Multiinstitutional epidemiological study regarding osteoarthritis of the hip in Japan

SEIYA JINGUSHI[1], SATOKO OHFUJI[2], MUROTO SOFUE[3], YOSHIO HIROTA[2], MORITOSHI ITOMAN[4], TADAMI MATSUMOTO[5], YOSHIKI HAMADA[6], HIROYUKI SHINDO[7], YOSHIO TAKATORI[8], HARUMOTO YAMADA[9], YUJI YASUNAGA[10], HIROSHI ITO[11], SATOSHI MORI[12], ICHIRO OWAN[13], GENJI FUJII[14], HIROTSUGU OHASHI[15], YUKIHIDE IWAMOTO[16], KEITA MIYANISHI[1], TOSHIRO IGA[3], NAONOBU TAKAHIRA[4], TANZO SUGIMORI[5], HAJIME SUGIYAMA[17], KUNIHIKO OKANO[7], TATSURO KARITA[18], KENICHI ANDO[9], TAKANARI HAMAKI[10], TERUHISA HIRAYAMA[11], KEN IWATA[19], SATOSHI NAKASONE[13], MASANORI MATSUURA[15], and TARO MAWATARI[16]

[1] Department of Orthopaedic Surgery, Kyushu Rosai Hospital of Japan Labor Health and Welfare Organization, 1-3-1 Takamatsu Kuzuhara, Kokura-minami-ku, Kitakyushu 800-0296, Japan
[2] Department of Public Health, Osaka City University Graduate School of Medicine, Osaka, Japan
[3] Orthopaedic Division, Nakajo Central Hospital, Niigata, Japan
[4] Department of Orthopedic Surgery, School of Medicine, Kitasato University, Sagamihara, Japan
[5] Department of Orthopaedic Surgery, Kanazawa Medical University, Uchinada, Japan
[6] Orthopaedic Division, Mitsuwadai General Hospital, Chiba, Japan
[7] Department of Orthopaedic Surgery, Graduate School of Medicine, Nagasaki University, Nagasaki, Japan
[8] Division of Science for Joint Reconstruction, Graduate School of Medicine, The University of Tokyo, Tokyo, Japan
[9] Department of Orthopaedic Surgery, Fujita Health University School of Medicine, Toyoake, Japan
[10] Department of Artificial Joints and Biomaterials, Graduate School of Biomedical Sciences, Hiroshima University, Hiroshima, Japan
[11] Department of Orthopaedic Surgery, Asahikawa Medical College, Asahikawa, Japan
[12] Department of Bone and Joint Surgery, Seirei Hamamatsu General Hospital, Hamamatsu, Japan
[13] Orthopedic Surgery, Department of Clinical Neuroscience, School of Medicine, University of the Ryukyus, Nishihara, Japan
[14] Tohoku Hip Joint Center, Matuda Hospital, Sendai, Japan
[15] Department of Orthopedic Surgery, Saiseikai Nakatsu Hospital, Osaka, Japan
[16] Department of Orthopaedic Surgery, Clinical Medicine, Graduate School of Medical Sciences, Kyushu University, Fukuoka, Japan
[17] Interdisciplinary Graduate School of Medicine and Engineering, University of Yamanashi, Chuo, Japan
[18] Orthopaedic Surgery, Sensory and Motor System Medicine, Surgical Sciences, Graduate School of Medicine, The University of Tokyo, Tokyo, Japan
[19] Department of Orthopaedic Surgery, Kagawa University Faculty of Medicine, Miki, Japan

Abstract

Background. Osteoarthritis (OA) of the hip is a major disease that affects the healthy lifespan of a population. It is necessary to fully understand the patients' conditions before a systematic treatment can be applied. However, a nationwide epidemiological study regarding hip OA has not yet been conducted in Japan. The present study examined the current status of patients with hip OA, including the disease etiology.

Methods. This is a multiinstitutional study of new patients presenting with hip OA at the orthopedic outpatient clinics of 15 institutions in five geographical areas of Japan. The collected data from each patient included the sex, age, treatment history for developmental dysplasia of the hip (DDH), the clinical score of the hip joints based on the Japanese Orthopaedic Association (JOA) scoring system, and the pelvic inclination according to anteroposterior radiographs. In addition, the etiology was determined from the following 17 options: primary OA, acetabular dysplasia, intragluteal dislocation, osteonecrosis, trauma, Perthes disease, slipped capital femoral epiphysis, infection, rheumatoid arthritis, ankylosing spondylitis, neuroarthropathy, endocrine diseases, metabolic diseases, hereditary bone diseases, synovial chondromatosis, generalized OA, and others.

Results. There were a substantially larger number of female patients than male patients. This difference regarding sex was present in each generation. The mean age of the patients was 58 ± 14 years. The peak age at presentation was approximately 50 years. Most patients had no history of therapy for DDH. The older patients had lower gait and activities of daily living scores. The etiology was assessed to be acetabular dysplasia in most of the patients. A lower frequency of elderly patients demonstrated acetabular dysplasia. The patients who had a pelvic posterior inclination increased with increasing age.

Conclusions. The patients with hip OA in Japan were unique in regard to age distribution, sexual heterogeneity, and disease etiology.

Offprint requests to: S. Jingushi
Received: January 13, 2010 / Accepted: May 6, 2010

Introduction

Osteoarthritis (OA) of the hip is a major disease that affects the healthy lifespan of a population. It is necessary to understand the patients' condition before systematic treatment can be applied. However, a nationwide

epidemiological study regarding OA of the hip has not yet been conducted in Japan, based on the current literature. In addition, the etiology has been thought to be unique in Japan, and most OA hips were thought to be secondary to acetabular dysplasia. This was mainly due to developmental dysplasia of the hips (DDH) during infancy. Currently, there are few DDH patients because prophylaxis, such as improved directions for putting on diapers, have been carried out. This may result in a change in the etiology of hip OA in Japan.

Therefore, we planned a study to investigate patients with hip OA in many institutions located throughout Japan. Many types of data were collected, including information both about each patient and about each hip joint such as the measurements and stage in the radiograph. In this report, we focused on the data regarding each patient, and herein report the current status of patients with hip OA in Japan, including an investigation of the disease etiology.

Patients and methods

The present study was a multiinstitutional examination of the patients with hip OA. Data were collected from the patients who were newly admitted to the orthopedic outpatient clinic of each institution. The patients were limited to those old enough to have hip joints that had completed closure of the growth plate. The patients were excluded if they had undergone an operation on both hip joints after growth plate closure. Osteoarthritis of the hip was defined as a symptomatic hip joint that had radiological osteoarthritic changes, such as joint space narrowing, sclerotic changes of the subchondral bone, osteophyte formation, or a bone cyst. A symptomatic hip joint that had a deformity in the joint, such as acetabular dysplasia or dislocation, but no osteoarthritic changes was also included.

Data were collected for 9 months after the study had received approval from the institutional review board including the one of the first author's institution. Fifteen institutions in five areas of Japan participated in this study. In the Kyushu and Okinawa areas, data from 158 patients (33%) were collected from four institutions. In the Shikoku, Chugoku, and Kinki areas, the data from 98 patients (20%) were collected at two institutions. In the Chubu area, the data from101 patients (21%) in three institutions were collected. In the Kanto area, the data were collected from 109 patients (22%) in three institutions. In the Tohoku and Hokkaido areas, data were collected from19 patients (4%) in three institutions. Written informed consent was obtained from each patient.

The collected data from each patient included the sex, age, treatment history for DDH, body mass index (BMI), and the clinical score of the hip joints based on the Japanese Orthopaedic Association (JOA) scoring system. The score was based on pain (40 points), range of motion (20), gait (20), and activities of daily living (ADL) (20).[1] In addition, the etiology was assessed by the hip surgeon at each institution from the following 17 potential etiologies: primary OA, acetabular dysplasia, intragluteal dislocation, osteonecrosis, trauma, Perthes disease, slipped capital femoral epiphysis, infection, rheumatoid arthritis, ankylosing spondylitis, neuroarthropathy, endocrine diseases, metabolic diseases, hereditary bone diseases, synovial chondromatosis, generalized OA, and others.

The pelvic tilt was calculated based on measurements from radiographs of the bilateral hip joints according to a previous report.[2] Briefly, the sagittal pelvic tilt was calculated from the radiological shape of the pelvic cavity using the equation: $A = -67.0^\circ \times L/T + 55.7^\circ$ in males and $A = -69.0^\circ \times L/T + 61.6^\circ$ in females according to the longitudinal/transverse axis length (L/T) ratio of the radiological shape of the pelvic cavity on the anteroposterior (AP) radiograph. The equation was developed by comparing the degree of the sagittal pelvic tilt to the L/T ratio using human pelvic bones. According to an original study using radiographs of normal hip joints, the standard pelvic angle was $19.47^\circ \pm 6.26^\circ$ in males and $19.97^\circ \pm 5.93^\circ$ in females. When the pelvic angle was $>20^\circ$, the pelvis was defined as having a posterior tilt.

The patient's characteristics, including etiology, were compared across age categories using a Kruskal-Wallis test (continuous variables) and a Mantel-Haenszel chi-squared test (categorical variables). For the comparisons across sexes, a Wilcoxon rank sum test and a chi-squared test were performed. All analyses were performed using a Statistical Analysis System, Version 9.1 software program (SAS Institute, Cary, NC, USA). Differences with $P < 0.05$ were considered statistically significant.

Results

A total of 485 patients were examined, with 433 (89%) female and 52 (11%) male patients. The mean age was 58 ± 14 years (median age 59 years, range 15–85 years). The number of the patients in each generation peaked when they were in their fifties. Most patients were in their fifties (27%), sixties (23%), and seventies (21%) at the time of presentation. Young patients (<50 years old) were also included (24%) (Fig. 1).

The mean BMI was 23.4 ± 3.7. The mean BMI of female patients (23.3 ± 3.6) was lower than that of male patients (24.8 ± 3.9) ($P = 0.003$, Wilcoxon rank sum test). The percentage of obesity (BMI ≥ 25.0) among female patients (26%) was significantly lower than that

among male patients (48%) (P = 0.002, chi-squared test).

Many patients (72%) had no past history of treatment for DDH. Only 19 patients (4%) had previously undergone operative treatment, whereas others (24%) had received conservative treatment during their childhood. During every decade of patient age, the patients who had no past history of DDH treatments were present at a larger proportion than those who had undergone DDH treatments (Fig. 2). The older the patient was, the less the proportion of patients with a past history of DDH ($P < 0.001$).

The proportion of patients who had bilateral hip OA was 56%. The older the patient was, the lower this proportion (P = 0.0002) (Table 1). The mean JOA scores for patient gait and ADL were 12 ± 5 and 14 ± 4, respectively. The correlation coefficients between the age and the gait score and between the age and the ADL score were –0.46 ($P < 0.0001$) and –0.50 ($P < 0.0001$), respectively. The older patients tended to have lower gait and ADL scores.

The etiology for hip OA was determined to be acetabular dysplasia for most patients (Table 2). Primary OA was secondary (9%), and the proportions of the other etiology options were all <2%. This distribution in etiology was significantly different in female patients from that in male patients ($P < 0.0001$). In addition, the proportion of acetabular dysplasia among female patients was significantly higher than that in male patients ($P < 0.0001$, chi-squared test). The older the patients were, the lower the proportion of acetabular dysplasia was ($P < 0.0001$) (Fig. 3). An etiology of primary OA was present for 18% and 38% in the patients who presented in their seventies and eighties, respectively. The correlation coefficient between the age and the pelvic inclination angle was 0.42 ($P < 0.0001$), and the pelvic inclination angle increased with advancing age ($P < 0.0001$). The proportion of the patients who had a posterior pelvic tilt also increased with increasing age ($P < 0.0001$) (Table 3).

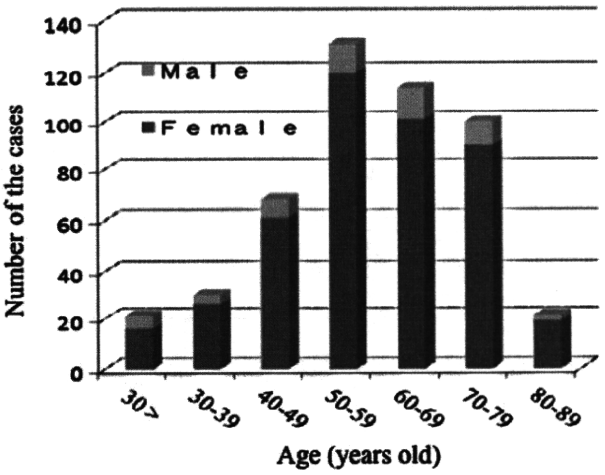

Fig. 1. Age distribution of the patients

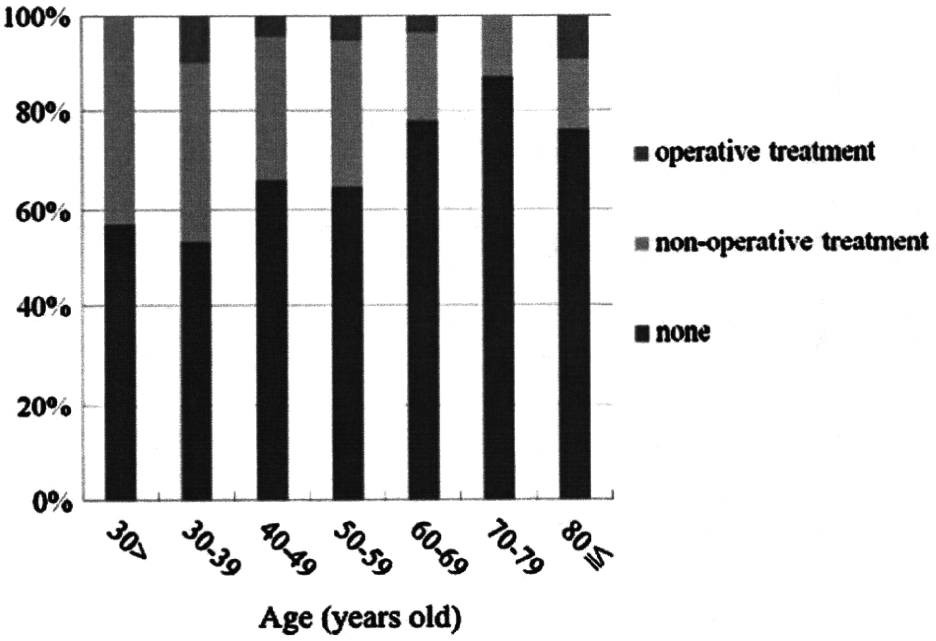

Fig. 2. Proportion of patients who had no history of treatment for developmental dysplasia of the hip. The proportion decreased with decreasing patient age (chi-squared test: $P < 0.001$)

Table 1. Involved side and the clinical scores, by the age of the patients

Parameter	<30 Years	30–39 Years	40–49 Years	50–59 Years	60–69 Years	70–79 Years	≥80 Years	*P*
No. of cases	21	30	68	131	114	100	21	
Involved side (no.)								
Hemilateral	8 (38%)	7 (23%)	24 (35%)	53 (40%)	57 (50%)	54 (54%)	13 (62%)	0.0002*
Bilateral	13 (62%)	23 (77%)	44 (65%)	78 (60%)	57 (50%)	46 (46%)	8 (38%)	
Clinical score								
Gait[a]	17.2 ± 3.4	17.0 ± 2.6	12.8 ± 4.3	12.6 ± 4.2[#]	11.0 ± 5.0	9.8 ± 4.3	6.2 ± 4.2	<0.0001**
ADL[a]	18.8 ± 2.0	17.8 ± 3.0	15.2 ± 3.9	14.3 ± 3.5	13.4 ± 3.7	11.6 ± 3.4	10.0 ± 2.8	<0.0001**

ADL, activities of daily living
[a] Mean ± SD
* Mantel-Haenszel chi-squared test
** Kruskal–Wallis test
# One case was unknown

Table 2. Etiology for osteoarthritis of the hip

Etiology[a]	Total (n = 485)	Male (n = 52)	Female[c] (n = 433)
Primary OA	44 (9%)	9 (17%)	35 (8%)
Acetabular dysplasia	390 (81%)	29 (56%)	361 (84%)
Others	48 (10%)	14 (27%)	34 (8%)
Bilateral OA of the hip withdifferent etiologies[b]	3 (1%)	0	3 (1%)

OA, osteoarthritis
[a] There were no cases of the following etiologies: slipped capital femoral epiphysis, neurological arthropathy, synovial chondromatosis
[b] All of the left hips had acetabular dysplasia. In the right hips, there were one and two cases of primary OA and intragluteal dislocation, respectively
[c] The difference between the etiologies in male and female patients was significant (P = 0.0001, chi-squared test)

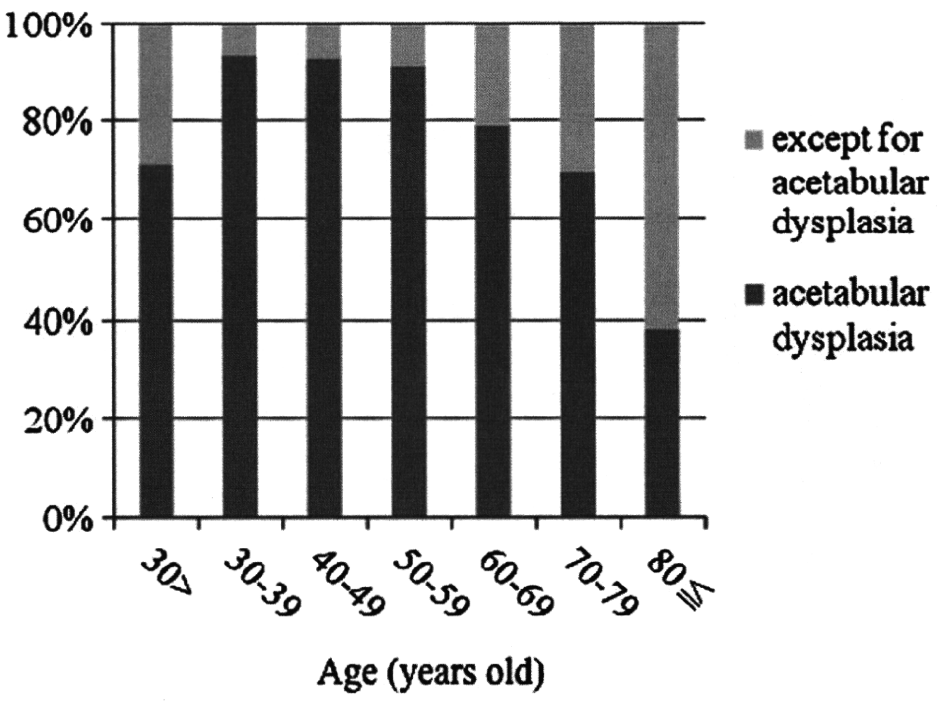

Fig. 3. Proportion of patients in whom it was determined that acetabular dysplasia was the disease etiology. The proportion decreased with decreasing patient age (chi-squared test: $P < 0.0001$)